Formability Analysis of Sheet Metals Using Machine Learning

Technical Report

April 11, 2023

Submitted to-

Prof. Shamik Basak
Mechanical and Industrial Engineering Department
Indian Institute of Technology Roorkee

Submitted by-

Ansh Saini (20113029),
Bakshi Hrishikesh Shirish (20117037),
Deepak Sharma (20113046),
Harsh Pal (20117057),
Shreya Singh(201170119)

B. Tech Mechanical Engineering (3rd year)
Mechanical and Industrial Engineering Department
Indian Institute of Technology, Roorkee

Table of Content

List of Figures

Acknowledgement

We would like to extend our sincere gratitude to all those who have contributed to the success of this project. Firstly, we would like to express our thanks to our professor Dr. Shamik Basak Sir for his guidance, insights, and unwavering support throughout the project. His expertise and mentorship have been instrumental in shaping our project.
We also want to thank Mr. Abdul Sir (Ph.D. Student at IIT Roorkee) for his valuable insights in completing the project. Finally, we would like to acknowledge the contribution of our batchmates who helped us with the project.
We are grateful to have had the opportunity to undertake this project.

Abstract

In sheet metal industries, predicting and avoiding failures, such as necking, fracture, and wrinkling, is important. Thus, working within a safe region to avoid these failures is important. The forming limit diagram (FLD) is the most appropriate tool to obtain the safe strain region for every sheet metal in different conditions. Forming Limit Diagram of perforated sheet metal can be affected by its mechanical properties like Yield Strength, Sheet thickness, Anisotropy value, Ultimate Tensile Strength, Strain Hardening exponent, and total elongation. In this project, the mechanical properties of aluminium and steel metal sheets are correlated with their forming limit diagram at room temperature. Various models based on machine learning and deep learning have been introduced to reveal the forming limit diagram of various metal sheets and then the accuracy of different models was compared to select the best model. The effect of each mechanical property on the FLD was also studied and analysed. After using experimental data to train and validate the various models, the models were applied to the test data for the prediction of forming limit diagrams.

Introduction

The formability of sheet metal and the optimization of the load curve are very important aspects of manufacturing process design. During forming these sheets are subjected to various types of strain. When the strain reaches/exceeds a critical value, different types of failures, namely, necking, fracture, and wrinkling occur. Therefore, the estimation of material formability plays a key role in evaluating the workability of sheet metals and diagnosing production problems in the forming processes. Forming limit diagram (FLD) is commonly used to experimentally characterize the formability of sheet metals. 1. A typical FLD shows the major in-plane strain on the vertical axis and the minor in-plane strain on the horizontal axis. FLD provides a tool for the determination of whether a given forming process will result in failure or not. Such information is critical in the design of forming processes and is, therefore, fundamental to the design, as well as optimization and problem corrections in the manufacturing process. Forming Limit Curve (FLC) is a line on FLD which divides safe levels of strains from unsafe ones. denotes the lowest point of the FLC which lies near the plane-strain state. Limit strains in FLC can be higher than tensile uniform elongation because the geometrical constraints prevent diffuse necking during biaxial sheet deformation. The FLD is also very useful in finite element method (FEM) analysis, die design optimization, die tryout, and quality control during production. FLC is experimentally determined by conducting hemispherical/flat-bottom punch stretching tests up to the onset of necking on gridded blanks. The experimental strain measurement procedure from the gridded sample is costly and laborious and it involves both skill and care to determine accurate FLC. Consequently, analytical and numerical procedures to determine FLC are developed, but the accuracy of those procedures is not sufficient to rely on them. In today's world where every industrial domain is using ML/AI in some or another way, we have used ML models to predict the FLDs of steel and aluminum sheet metals while considering the mechanical properties and the thickness of the metal sheet as the input features for the models. A schematic of FLD is illustrated in Fig. 1.

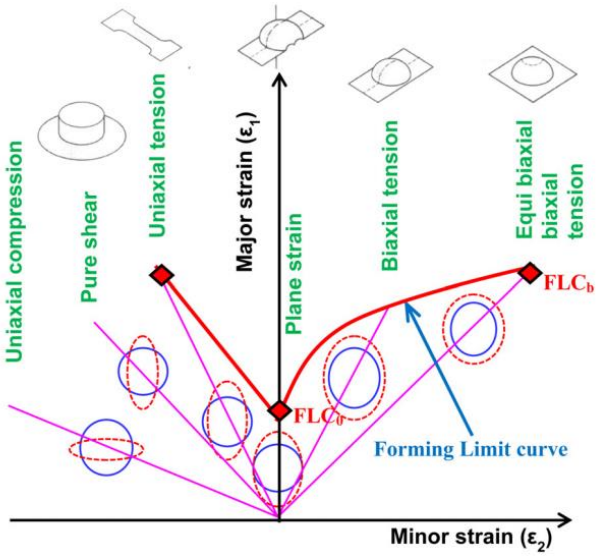

Figure 1: Schematic diagram of forming limit diagram (FLD) indicating nature of deformation

Methodology

The methodology is to extract the create a dataset that includes experimental Forming Limit Curve (FLC) and tensile properties (UTS, YS, n, r, t, ε_t) of various steel and aluminium sheets from the literature. After extraction, data will be pre-processed and will be used to train different machine learning models.

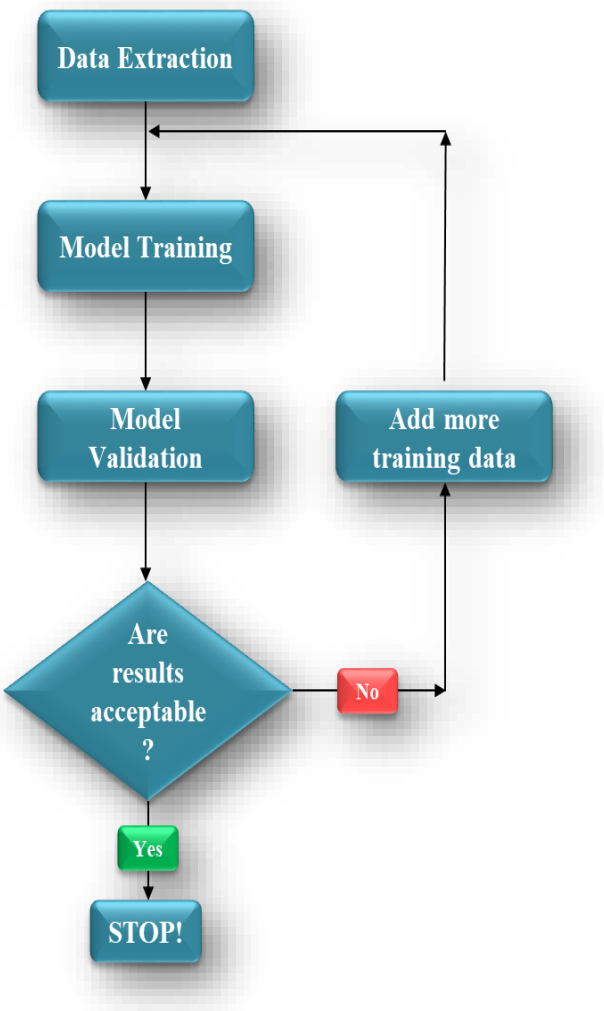

Figure 2: Workflow Chart

Experimental Data Collection

Material Selection

For the project at hand, a variety of steel and aluminium grades were chosen from various sources available on the internet. Each of these materials has its own unique chemical composition, which can significantly affect their properties and performance. However, to predict the forming limit diagram for these materials, the chemical composition has not been considered and has instead been neglected. This decision was made to simplify the prediction process and reduce the number of variables that need to be considered. As a result, the focus of the project has been on other factors that are known to affect the forming limit diagram, such as the mechanical properties and processing conditions of the materials. By analysing these factors, it is hoped that valuable insights can be gained into the behaviour of these materials during the forming process, which could ultimately help to improve the design and manufacturing of metal components.

Material Properties

For subsequent analysis, experimental data has been gathered from a variety of published literature sources, as indicated in the references. The data has been collected for a wide range of steel and aluminium grades, with a focus on collecting information about their tensile properties and sheet thickness. Specifically, the collected tensile properties include the Strain Hardening Exponent , Coefficient of Normal Anisotropy, Yield Stress, Ultimate Tensile Stress, and Total Tensile Strain. Meanwhile, the sheet thickness is denoted by 't' the variable and is measured in millimetres.

The collected steel grades comprise various types, such as interstitial-free (IF), deep drawn (DD), bake hardened (BH), micro-alloy (MA), dual-phase (DP), transformation-induced plasticity (TRIP), and twin-induced plasticity (TWIP) steels. On the other hand, the collected aluminium grades include AA2024, AA5083, AA1050-O, AA1050-H, and other similar grades. By gathering this diverse set of data, it is hoped that a comprehensive analysis can be performed to better understand the mechanical behaviour of these materials and their suitability for various applications.

Extraction of Data from FLDs

The published journal papers were used as the source for extracting additional data, which involved a few steps. Firstly, an online tool called "Web-Plot Digitiser" was utilized to extract the coordinates of the point FLC_O, which represents the forming limit for the plane strain condition ($\alpha = 0$), from the graph. After that, four points located on the right side of FLC_O and three points on the left side of FLC_O were extracted from the same Forming Limit Curves, each point being at equal intervals. These points were then recorded and tabulated in a table for further analysis. The four points on the right side were collected based on the ratio of $\varepsilon_2/\varepsilon_1$, which were 1, 0.75, 0.5, and 0.25 respectively, while the three points on the left side were collected based on the ratio of $\varepsilon_2/\varepsilon_1$, which were -0.17, -0.33, and -0.5.

The experimental data that have been collected will serve a significant purpose of establishing correlations and validating models. These correlations and models will be of great importance in providing a deeper understanding and explanation of the data obtained. Therefore, the collected experimental data will be utilized to create strong relationships between different variables and to verify the accuracy and reliability of the models that have been developed.

Paper	Material	Material Properties						FLCo (E2/E1~0)		(E2/E1~1)	
Number	Type	Sheet Thickness (t) (mm)	Strain Hardening (n)	Anisotropy Value (r)	YS(N/mm2)	UTS(N/mm2)	Total tensile Strain (Et)	E1- Major	E2 - Minor	E1 - Major	E2 - Minor
S18	EDD	0.80	0.25	1.19	195.40	321.80	0.39	0.350	-0.006	0.823	0.821
S18	EDD	1.00	0.17	1.01	245.00	325.10	0.31	0.320	-0.001	0.742	0.740
S18	EDD	1.25	0.21	1.56	223.80	303.40	0.39	0.283	-0.003	0.646	0.642
S18	EDD	1.60	0.25	1.58	188.90	299.40	0.45	0.231	-0.001	0.515	0.512
S18	EDD	2.00	0.22	1.37	202.80	276.80	0.42	0.172	-0.013	0.374	0.324
S9	DQ	0.81	0.24	1.11	180.00	313.00	0.41	0.440	0.000	0.597	0.486
S9	DQ	0.81	0.23	1.21	188.00	308.00	0.43	0.440	0.000	0.572	0.456
S9	DQ	0.91	0.20	1.28	201.00	316.00	0.38	0.390	0.000	0.563	0.452
S9	DQSK	0.94	0.20	1.47	190.00	321.00	0.38	0.370	0.000	0.550	0.430
S9	DQSK, G90	0.71	0.20	1.51	207.00	300.00	0.33	0.370	0.000	0.487	0.376
S9	DQSK, G60	0.76	0.19	1.80	200.00	308.00	0.37	0.410	0.000	0.578	0.496
S9	DQSK, A40	0.94	0.17	1.40	197.00	310.00	0.38	0.410	0.000	0.576	0.477
S9	DQSK, G60	0.81	0.17	1.67	185.00	286.00	0.41	0.430	0.000	0.590	0.475
S9	DQSK, G60	0.76	0.22	1.52	182.00	304.00	0.42	0.440	0.000	0.597	0.486
S9	DQSK, G60	0.86	0.20	1.34	197.00	311.00	0.43	0.415	0.000	0.581	0.456
S9	DQSK, G60	0.69	0.20	1.63	181.00	276.00	0.42	0.425	0.000	0.587	0.477

Figure 3: *Dataset* (*Link*)

Data Pre-Processing & Cleaning

The collected dataset, which was intended for use in training various machine learning models, underwent a thorough cleaning and pre-processing procedure prior to utilization. This process involved removing any outliers present in the data through data cleaning techniques, as well as replacing any null values with the most appropriate corresponding values using data pre-processing methods. The next task was to understand the correlation of input features with each other. This was done using the Pearson-Correlation Matrix that showed that Yield Strength and Ultimate Tensile Strength are highly correlated with each other with a value of 0.96. So, Ultimate Tensile Strength has been removed as the input feature.

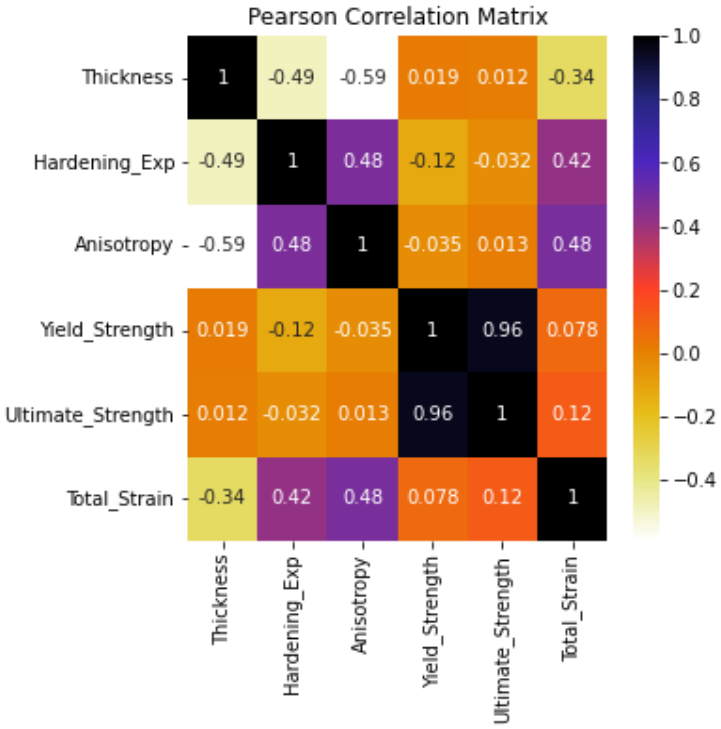

Figure 4: Pearson – Correlation Matrix indicating correlation between input features

Furthermore, to ensure optimal performance of the machine learning models during the training and validation stages, all dataset columns used for predicting FLD using these models underwent scaler normalization. This was done to account for the differences in the ranges and units of input feature values, ensuring that they were appropriately standardized before being passed through the models.

Trends in the Data

The 5 input features are independently used to find their variation with the minimum point in the FLD curve i.e., the FLC_O value corresponding to the plane strain. For this 4 machine learning techniques – Linear Regression, Linear Support vector Regression, Random Forest Regression, and Artificial Neural Network are used. All the input features are best fitted with the ANN model with an R^2 value being more than 0.65. The Random Forest Regressor also gave a good result with an R^2 value lying between 0.6 to 0.65.

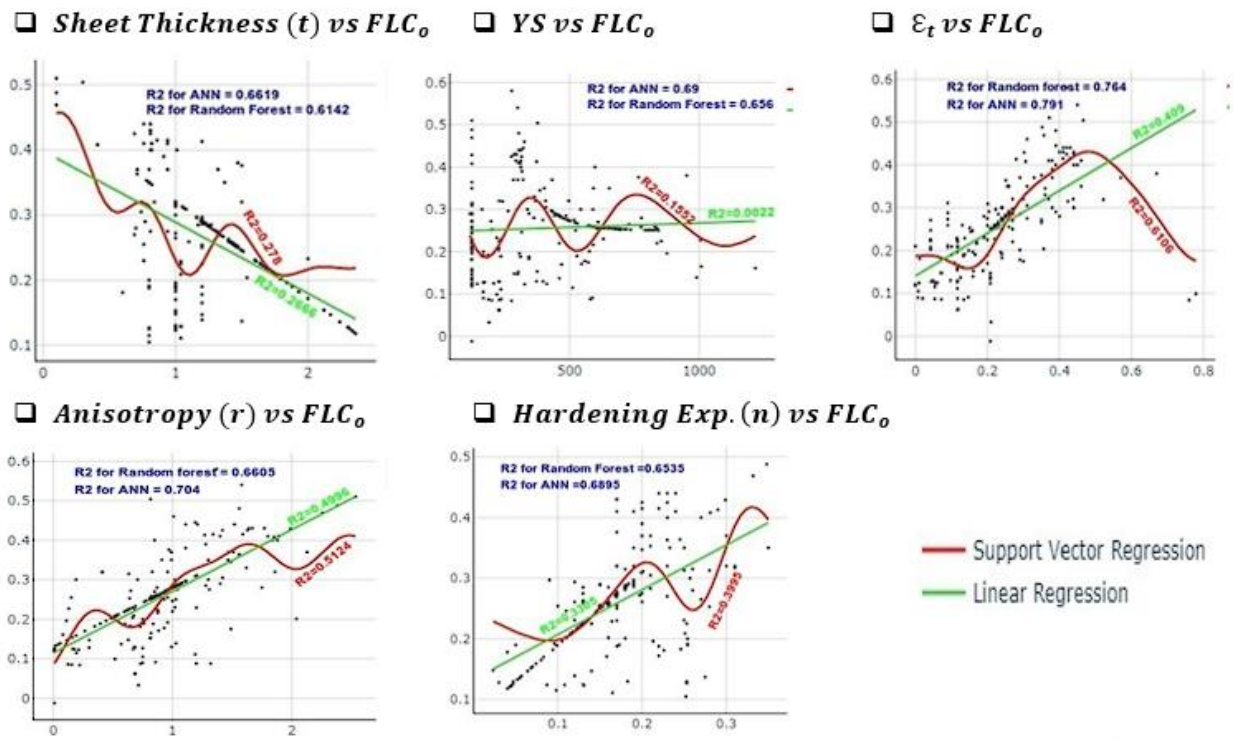

Figure 5: Variation of Input Features with FLC_o

Model Architecture

The ML models which we have employed for the FLD prediction are – Linear regression, Support Vector Regression, Random Forest, and Artificial Neural Network. For tuning the models, the dataset has been divided into training and testing in 85% and 15% respectively. For the ANN model, the test data has been further divided into validation data and testing in 40% and 60% respectively.

Linear Regression

Linear regression is a statistical modelling technique used to establish a relationship between a dependent variable (Y) and one or more independent variables (X) by fitting a linear equation to the observed data. The goal of linear regression is to find the best-fit line that can represent the relationship between the variables.

The equation for simple linear regression model is:

$$y(x) = \beta + a * x + \varepsilon$$

where:
Y is the dependent variable or the response variable.
X is the independent variable or the predictor variable.
B and α are the regression coefficients or the intercept and slope of the line, respectively.
ε is the error term or the residual, which represents the difference between the observed and predicted values.

Linear Support Vector Regression

Linear Support Vector Regression (SVR) is a variant of Support Vector Regression that uses a linear kernel function to map the input data to a high-dimensional feature space. Linear SVR aims to find a hyperplane that best separates the data into two regions - one for the target variable values that are greater than or equal to the predicted values, and one for the target variable values that are less than or equal to the predicted values. The points that lie closest to the hyperplane are called support vectors and are used to define the hyperplane.

Random Forest Regression

Random Forest Regression is a powerful and flexible algorithm that can handle a wide range of regression problems, including those with complex and non-linear relationships between the input and output variables. It is also able to handle missing data and noisy input features. It works by randomly selecting a subset of the training data and a subset of the input features to build each decision tree. This process is repeated to build multiple decision trees, each with different subsets of the data and features.

Artificial Neural Networks (ANN)

Artificial Neural Networks (ANNs) are a type of machine learning algorithm that are inspired by the structure and function of biological neurons in the brain. ANNs consist of interconnected layers of artificial neurons that are trained to learn complex patterns and relationships between the input and output data.

An ANN typically consists of three types of layers: input layer, hidden layer(s), and output layer. The input layer receives the input data, which is then passed through the hidden layer(s) to the output layer. Each neuron in the hidden and output layers receives input from the previous layer, performs a weighted sum of the input, applies an activation function, and passes the output to the next layer.

The weights of the connections between the neurons are adjusted during the training phase using a process called backpropagation. The goal of backpropagation is to minimize the difference between the predicted output and the actual output by adjusting the weights of the connections.

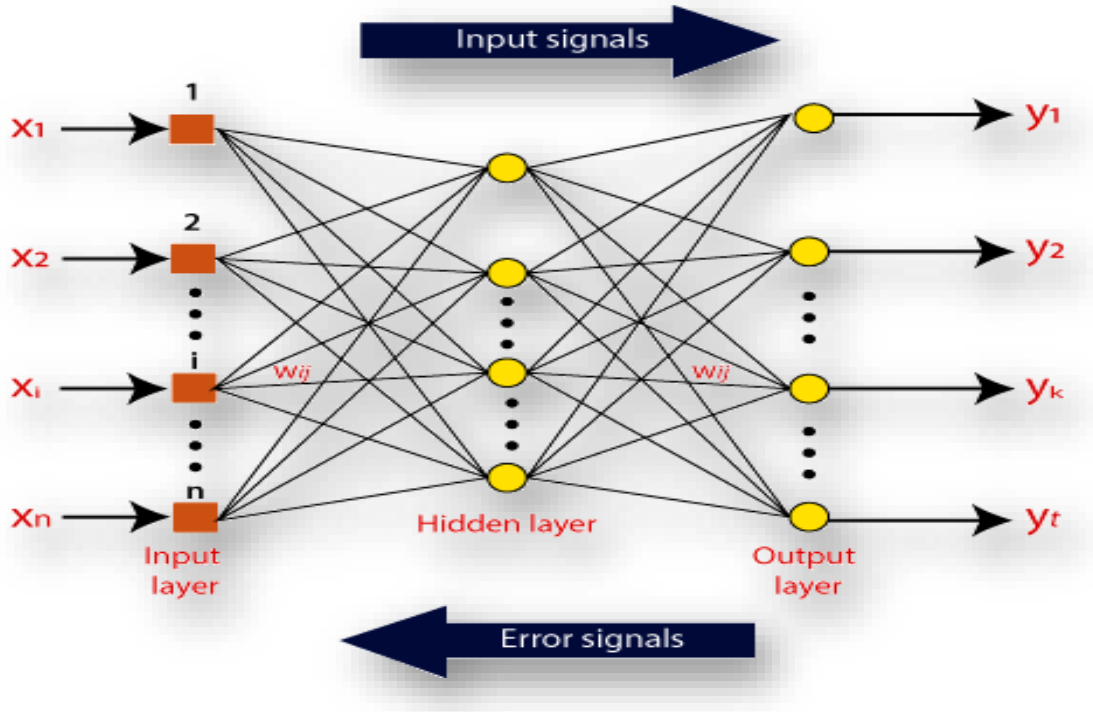

Figure 6: ANN Architecture

For this project, the ANN model has been built using three layers, with 32 units in two layers and 16 units in the output layer. The activation function used is the sigmoid function.

$$f(x) = 1/(1 + e^{-x})$$

Results

1. Linear Regression gave a R^2 value of 0.2417 on the test data.
2. Linear Support Vector Regression in a wrapper form with MultipleOutputRegressor showed good fitting on test data with a R^2 value of 0.3263.
3. The Random Forest Regressor model that works by building multiple decision trees, showed a much better R^2 value of 0.3884 on the test data.
4. The ANN was trained for 1000 epochs and on the test data the mean absolute error was 0.051 and the R^2 value was found to be 0.7182.

   On basis of the R^2 value, it is found that:

   $$ANN \gg Random\ Forest > LinearSVR > Linear\ Regression$$

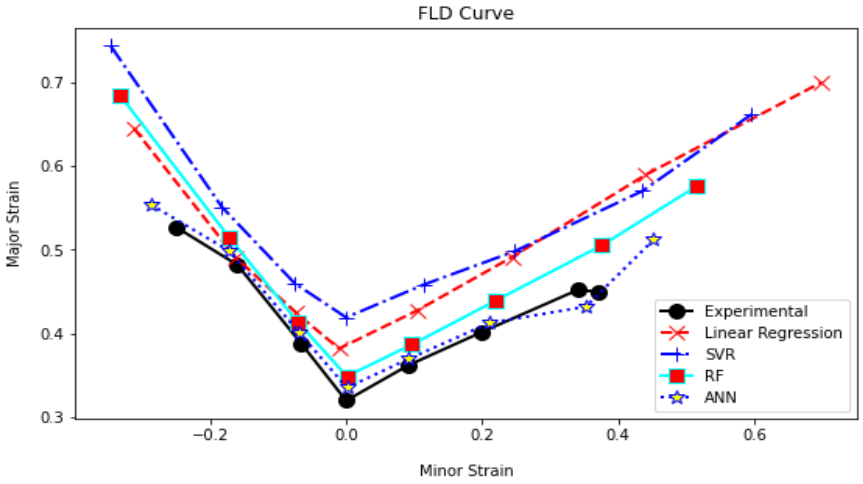

Figure 7: *Steel (IFHS) FLD*

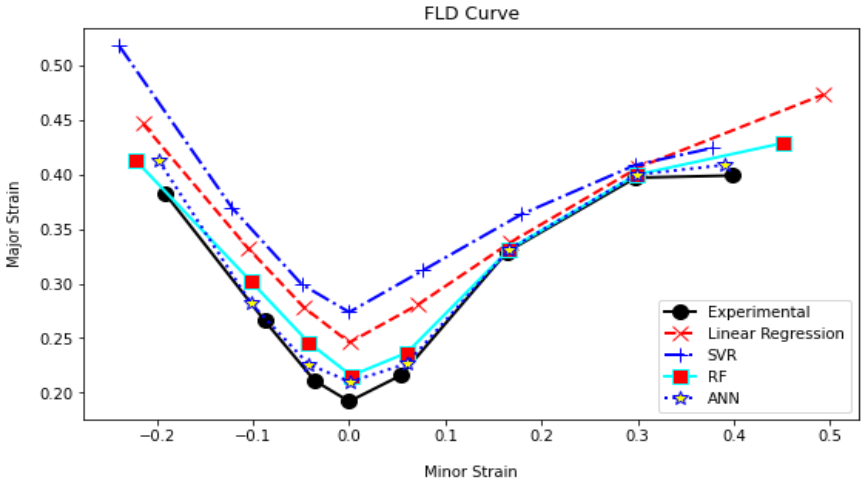

Figure 8: *Aluminium* (1100 − *H*24) *FLD*

Conclusions

The use of machine learning in forming limit curve (FLC) prediction faces several limitations. Despite extensive research, the available dataset for training an ANN model is limited, with only 221 entries. This is due to the difficulty in finding tabular data in the forming field. Additionally, the best model achieved an R^2 value of 0.7182 on the test data, which indicates room for improvement, provided there is more data. Another limitation is that the FLD is not solely dependent on material properties, but also on other factors like material composition, strain rate, pre-strain levels, and process parameters. These factors are neglected during FLD prediction, which leads to errors on the new dataset. Therefore, while models like ANNs have several advantages and a good accuracy, it is important to consider these limitations in the context of FLC prediction.

For future improvement, it is recommended to increase the number of dataset entries by performing more experimental procedures to establish FLD. Additionally, more advanced techniques and models, such as fuzzy logic, adaptive neural networks, and convolutional neural networks, can be applied to fit the dataset in a better way. These techniques may help

to improve the accuracy of FLC prediction and reduce the impact of the limitations discussed earlier.

References

1. A comparative study of the forming-limit diagram models for sheet steels
2. Finite Element Validation of Forming Limit Diagram of IN-718 Sheet Metal
3. Forming Limit Curves of Advanced High Strength Steels
4. Forming Limit Curve Determination of a DP-780 Steel Sheet
5. Polar effective plastic strain - forming limit diagram of DP 440 steel sheet with application to two-step forming test
6. The forming limit diagram of ferritic stainless-steel sheets: Experiments and modelling
7. Forming limit diagram of Advanced High Strength Steels (AHSS) based on strain-path diagram
8. Forming limit diagram prediction of 6061 aluminium by GTN damage model
9. Prediction of complete forming limit diagram from tensile properties of various steel sheets by a nonlinear regression-based approach
10. Experimental and theoretical formability analysis using strain and stress based forming limit diagram for advanced high strength steels
11. Formability limit diagrams of extra-deep-drawing steel at elevated temperatures
12. Prediction of forming limit in DP590 steel sheet forming: An extended fracture criterion
13. Theorical and experimental determination of the forming limit diagram for the AISI 304 stainless steel
14. Formability limits of high-strength H240LA steel sheets under stress/strain gradients
15. A new method of determining forming limit diagram for sheet materials by gas blow forming
16. Development of experimental and theoretical forming limit diagrams for warm forming of austenitic stainless steel 316
17. Determination of forming limit curve by finite element method simulations
18. Formability analysis of extra-deep drawing steel
19. Prediction of entire forming limit diagram from simple tensile material properties
20. Strain Hardening and Forming Limits of Automotive Steels
21. A study on fracture behaviour of three different high strength low alloy steel sheets during formation with different strain ratios
22. Formability of TWIP (twinning induced plasticity) automotive sheets
23. Forming limit criterion for ductile anisotropic sheets as a material property and its deformation path insensitivity, Part II: Boundary value problems
24. Development of experimental and theoretical forming limit diagrams for warm forming of austenitic stainless steel 316
25. Prediction of forming limit diagrams using machine learning
26. A comparative study on determination of forming limit diagrams for industrial aluminium sheet alloys considering combined effect of strain path, anisotropy and yield locus
27. Forming Limit Diagram Generation of Aluminium Alloy AA2014 Using Nakazima Test Simulation Tool
28. Comparative analysis of forming limit diagram of Al 5052-H32 and Al 6063 T5
29. Forming Limit Stress Diagram Prediction of Aluminium Alloy 5052 Based on GTN Model Parameters Determined by In Situ Tensile Test
30. Strain distribution and failure mode in single point incremental forming (SPIF) of multiple commercially pure aluminium sheets

31. Thermal forming limit diagram (TFLD) of AA7075 aluminium alloy based on a modified continuum damage model: Experimental and theoretical investigations
32. Comparative analysis between stress- and strain-based forming limit diagrams for aluminium alloy sheet 1060
33. Modelling of forming limit diagram of perforated commercial pure aluminium sheets using artificial neural network
34. Experimental and numerical evaluation of forming limit diagram for Ti6Al4V titanium and Al6061-T6 aluminium alloys sheets
35. Formability prediction of AL7020 with experimental and numerical failure criteria
36. Predictions of Forming Limit Curves of AA6014 Aluminium Alloy at Room temperature
37. A new measurement technology for forming limit in aluminium alloy under biaxial dynamic loading
38. A method for stress space forming limit diagram construction for aluminium alloys
39. Experimental measurement and theoretical prediction of forming limit curve for aluminium alloy 2B06
40. Stress based forming limit diagram for formability characterization of 6061 aluminium
41. Influence of the post-necking prediction of hardening law on the theoretical forming limit curve of aluminium sheets
42. Forming limit curves analysis of aluminium alloy considering the through-thickness normal stress, anisotropic yield functions and strain rate
43. Forming-limit curves of aluminium and aluminium alloy sheets and effects of strain path on the curves
44. Effect of electromagnetic forming heat treatment process on mechanical and corrosion properties of 2024 aluminium alloy
45. Experimental measurement and theoretical prediction of forming limit curve for aluminium alloy 2B06
46. Construction of forming limit diagrams for AA 5754 and AA2024 Aluminium alloys
47. Forming limit analysis for two-stage forming of 5182-O aluminium sheet with intermediate annealing
48. Modelling the Forming Limit Diagram for Aluminium Alloy Sheets using ANN and ANFIS
49. Aluminium Alloy Sheet-Forming Limit Curve Prediction Based on Original Measured Stress–Strain Data and Its Application in Stretch-Forming Process
50. Mechanical properties, spring back, and formability of W-temper and peak aged 7075 aluminium alloy sheets: Experiments and modelling
51. Effect of microstructure and texture on forming behaviour of AA-6061 aluminium alloy sheet
52. Experimental and theoretical investigations of the forming limit of 5754O aluminium alloy sheet under different combined loading paths
53. Formability analysis of pre-strained AA5754-O sheet metal using Yld96 plasticity theory: Role of amount and direction of uniaxial pre-strain
54. Failure strains of anisotropic thin sheet metals: Experimental evaluation and theoretical prediction
55. Microstructure, forming limit diagram, and strain distribution of pre-strained DP-IF steel tailor welded blank for auto body application